Available online at www.sciencedirect.com

SciVerse ScienceDirect

Ceramics International 39 (2013) 8293–8299

CERAMICS INTERNATIONAL

www.elsevier.com/locate/ceramint

Flower-like hydroxyapatite nanostructure obtained from eggshell: A candidate for biomedical applications

G. Suresh Kumar, E.K. Girija*

Department of Physics, Periyar University, Salem 636011, India

Received 3 January 2013; received in revised form 14 March 2013; accepted 22 March 2013
Available online 10 April 2013

Abstract

We report the apatite forming ability, biocompatibility, drug adsorption/desorption behavior, antibacterial activity and photoluminescence property of flower-like hydroxyapatite (HA) nanostructure which was obtained from eggshell biowaste via a simple and rapid microwave conversion process. The obtained results from the above studies indicate that the prepared flower-like hydroxyapatite nanostructure can be a potential material for the development of drug delivery carriers, bone substitutes and bioprobes.

Keywords: A. Microwave processing; C. Optical properties; D. Apatite; E. Biomedical applications; *In vitro* studies

1. Introduction

Hydroxyapatite ($Ca_{10}(PO_4)_6(OH)_2$, HA) is the main mineral constituent of calcified tissues such as bones and teeth. It has been widely used as a carrier for drug delivery, bone substitute for filling bone defects, scaffold matrix for tissue engineering and as a coating on biomedical implants owing to its excellent biocompatibility and bioactivity [1–3]. Not only the chemical composition of the HA phase but their morphology and size also have strong impact on the above biomedical applications [4–8]. Nanosized HA particles have better bioactivity and bioresorbability due to their large surface to volume ratio and unusual chemical/electronic synergistic effects [1,9]. Moreover, size and shape plays an important role on drug loading and releasing efficiency of HA [10–12]. Thus morphology and size dependent properties have a great interest and have been the topic of research interest for many years.

Over the past decades, a number of synthetic methods have been developed to synthesize HA nanocrystals with various sizes and morphologies [13–19]. Among the several routes, microwave irradiation is an efficient route, which provides rapid and facile procedure for synthesis of HA with variety of morphologies [17–20]. Organic modifiers such as cetyltrimethylammonium bromide (CTAB), citric acid and ethylene diammine tetra acetic acid (EDTA) which enable a facile control over the final shape and size of HA particles were often used in the microwave irradiation method [18–20]. In particular, EDTA was well demonstrated as an efficient crystal growth modifier for the synthesis of flower-like HA nanostructure [18].

On the other hand, everyday million tons of eggshells are being discarded as biowaste around the globe. Eggshell is a natural composite material consisting of calcium carbonate (94%), calcium phosphate (1%), organic matter (4%) and magnesium carbonate (1%) [21]. Important issues are minimization of this biowastes and recycling them into useful products. Recently, we have reported a simple and rapid microwave irradiation method for producing flower-like HA nanostructure from eggshell biowaste using EDTA as chelating agent [22]. In the present work, we have evaluated the apatite forming ability, biocompatibility, drug adsorption/desorption behavior, antibacterial activity and photoluminescence property of the flower-like HA nanostructure in order to check its applicability to different

*Corresponding author. Tel.: +91 9444391733; fax: +91 427 2345124.
E-mail address: girijaeaswaradas@gmail.com (E.K. Girija).

0272-8842/$ - see front matter © 2013 Elsevier Ltd and Techna Group S.r.l. All rights reserved.
http://dx.doi.org/10.1016/j.ceramint.2013.03.099

biomedical applications such as drug delivery, bone substitute and bioprobes.

2. Materials and methods

2.1. Preparation of flower-like HA nanostructure from eggshell biowaste

All the chemicals such as EDTA, di-sodium hydrogen phosphate (Na_2HPO_4), sodium hypochlorite (NaOCl) and sodium hydroxide (NaOH) were analytical grade obtained from Merck, India. The flower-like HA nanostructure (nHA) was synthesized from eggshell biowaste according to our previous report [22]. Briefly, eggshells were collected and immersed in boiling water to remove the inner membrane and impurities. After drying, they were ground into powder and immersed in sodium hypochlorite to remove organic components. Then, they were extensively washed with Millipore water and dried in vacuum oven for 5 h at 110 °C. 1 g of eggshell powder was then mixed with 0.1 M of EDTA solution to form Ca-EDTA complex. Subsequently, 0.06 M of Na_2HPO_4 solution was slowly added with obtained Ca-EDTA complex and stirred for 30 min. After stirring, pH of the reaction mixture was adjusted to 13 by using NaOH solution. Then, the prepared reaction mixture was kept in a microwave oven (2.45 GHz, 600 W, LG, India) and irradiated with microwave for 10 min. The obtained white precipitate was washed three times using Millipore water and dried at 110 °C in hot air oven for 5 h.

2.2. In vitro apatite forming ability in simulated body fluid (SBF)

The apatite forming ability of the nHA was studied by immersing the nHA disk in SBF at 37 °C. The SBF was prepared by dissolving appropriate amount of reagent grade NaCl, $NaHCO_3$, KCl, Na_2HPO_4, $MgCl_2 \cdot 6H_2O$, Na_2SO_4, $(CH_2OH)_3CNH_2$ and $CaCl_2 \cdot 2H_2O$ in deionized water. 1 M HCl was used to maintain pH of the solution at 7.4 to mimic the concentration of human blood plasma [23]. The as-synthesized nHA was pressed into disk by applying a pressure of ~24 MPa. Then, the disk was immersed in 30 ml of SBF in plastic containers with airtight lids at 37 ± 0.5 °C in an incubator. The SBF solution was renewed once in three days for a period of 21 days. Finally, the formation of bone-like apatite on the surface of nHA disk was analyzed by JEOL-6390 scanning electron microscope (SEM) with Oxford INCA energy dispersive X-ray fluorescence (EDX) microanalysis.

2.3. In vitro cell culture test

The biocompatibility of nHA with mouse fibroblast 3T3-L1 cells was determined by the MTT assay [24]. The mouse fibroblast 3T3-L1 was purchased from National Center for Cell Sciences (NCCS), Pune, India. For the MTT assay, the cells were grown in 25 cm^3 tissue culture flasks containing RPMI1640 medium as culture medium supplemented with 10% fetal calf serum, 100 U/ml penicillin, 100 μg/ml streptomycin and grown at 37 °C under a humidified atmosphere of 95% air and 5% CO_2. When cell density in culture flask reached 70–80% confluence, they were trypsinized and seeded in 96-well plates in the density of 2500 cells per well/100 μL and incubated for 24 h at CO_2 incubator. Then the as-prepared nHA at dosages 50, 100 and 200 μg ml^{-1} was dispersed in Dulbecco's Modified Eagle Medium (DMEM) and added to the cells. The plates were further incubated for 24, 48 and 72 hours in the CO_2 incubator.

After incubation, 50 μl of 3-(4,5-dimethylthiazol-2-yl)-2, 5-diphenyl tetrazolium bromide (MTT) solution (5 mg/ml in phosphate buffer saline (PBS)) was added into each well and the plate was further incubated for 150 min in incubator. After discarding the supernatants, the dark blue formazan crystals were dissolved in 100 μL dimethyl sulfoxide (DMSO) and the optical density was measured using Synergy H4 microplate reader at 570 nm. The mean and the standard deviation were obtained from sums of three different experiments.

2.4. In vitro drug adsorption and desorption study

Doxycycline hydrochloride ($C_{22}H_{24}N_2O_8$.HCl) was selected as the model drug and its chemical structure is shown in Fig. 1 [25]. Millipore water was employed as the solvent to prepare the drug solution.

In order to load the drug on nHA, 50 mg of as-prepared nHA was immersed in 10 ml drug solution containing 1 mg/ml doxycycline hydrochloride for a period of 24 h at room temperature. Then drug loaded nHA was separated by centrifugation (5 min, 2000 rpm) and dried at 60 °C for 12 h. Percentage of drug loading was calculated using the following equation: [26]

$$\text{Percentage of drug loading } \eta = \frac{C_0 - C}{C_0} \times 100$$

where C_0 and C represent the concentration of doxycycline hydrochloride in the solution before and after loading, respectively. To evaluate its *in vitro* release characteristics, drug loaded nHA was placed in a plastic container with 50 ml PBS of pH 7.4 at 37 ± 0.5 °C. The release medium was collected at various time intervals and the amount of drug released was determined using a Perkin Elmer lambda 25 UV–vis spectrometer. The concentration of doxycycline hydrochloride was calculated by employing a calibration curve.

2.5. Antibacterial activity

Antibacterial activity of as-prepared nHA and doxycycline hydrochloride loaded nHA was studied by standard disc diffusion

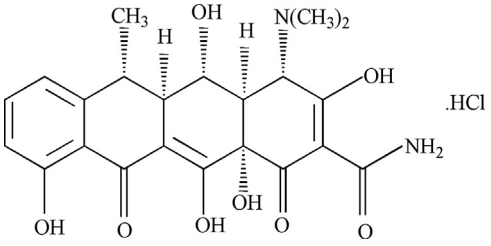

Fig. 1. Chemical structure of doxycycline hydrochloride.

method [17]. As-prepared nHA and doxycycline hydrochloride loaded nHA were pressed at ~24 MPa to form disk, each nominally 13.5 mm diameter and 2 mm thick. The micro-organisms such as *Escherichia coli* (Gram negative) and *Bacillus cereus* (Gram positive) were cultured on nutrient agar plates. After the culture, disks of pure nHA (control) and drug loaded nHA were located on this plate and incubated for 24 h at 37 ± 0.5 °C. The microbial inhibition zone excluding pellet was measured after the incubation period and its images were documented.

2.6. Photoluminescence study

The photoluminescence (PL) spectrum of the as-prepared nHA was obtained using Horiba Fluorolog FL3-22 spectrophotometer equipped with a 450 W xenon lamp as the excitation source.

3. Results and discussions

The synthesized product was confirmed to be Mg containing carbonated HA exhibiting flower-like morphology by XRD, FT-IR, SEM and EDX analysis [22]. Mg and carbonate were inherited from the eggshells, which were used as the calcium source for the synthesis. Moreover Mg and carbonate contents present in the synthesized nHA are similar to bone apatites [22,27,28].

Fig. 2(a) illustrates the SEM image of the surface of nHA disk before soaking in SBF, which indicates the presence of pores on the surface of nHA disk. Fig. 2(b–d) shows the SEM images of the surface of nHA disk after soaking in SBF for 21

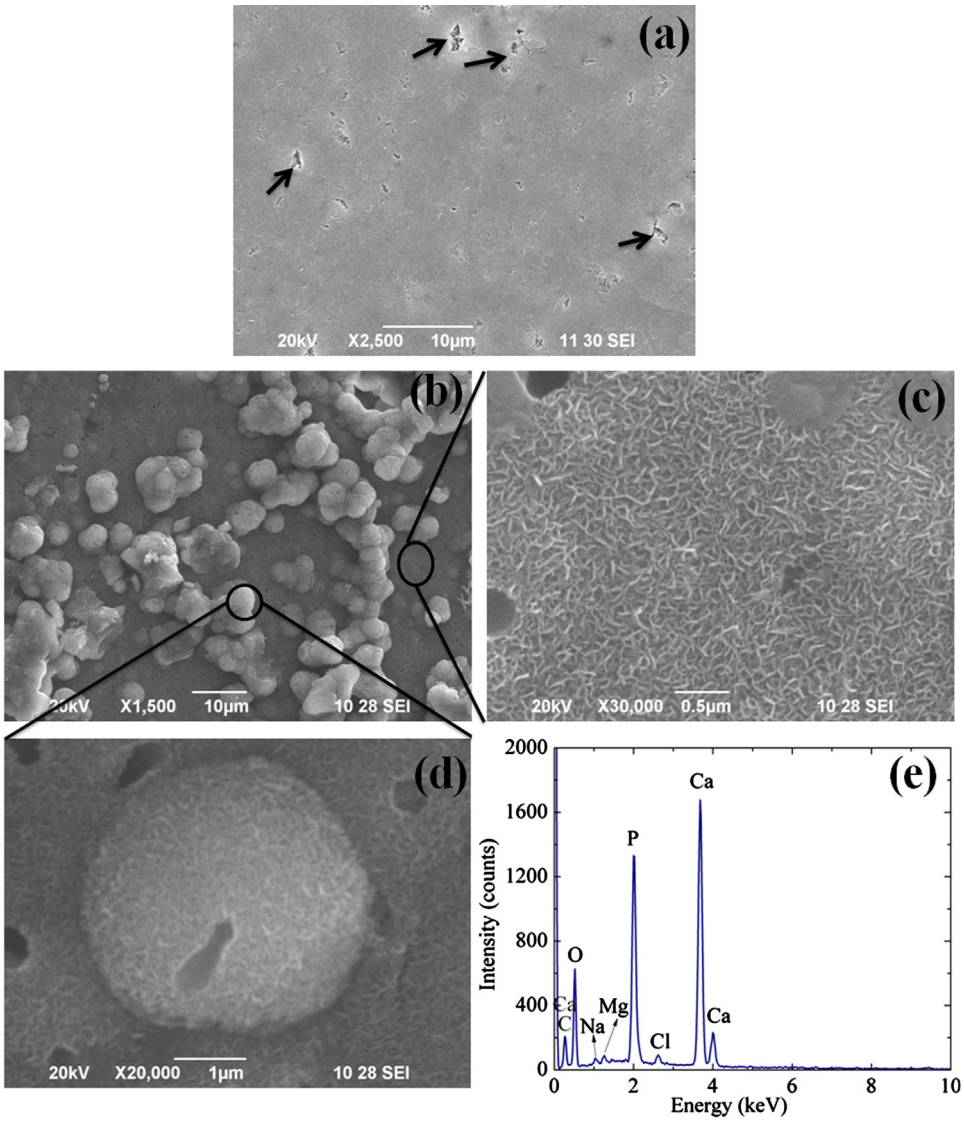

Fig. 2. SEM images of the surface of nHA disk (a) before, (b) after soaking in SBF for 21 days, (c) magnified view of apatite layer, (d) magnified view of spherical apatite deposits and (e) EDX spectrum of the apatite layer formed on the surface. Arrows in Fig. 2(a) indicate the presence of pores on the surface of nHA disk before immersion in SBF.

days. SEM observation revealed the formation of apatite layer with frequent aggregated spherical apatite deposits on the surface after immersion in SBF (Fig. 2(b)). Magnified views (Fig. 2(c) and (d)) depict flaky nanocrystals constituting the apatite layer as well as spherical apatite deposits. EDX spectrum (Fig. 2(e)) indicates the presence of Ca (23.93 wt.%), P (13.93 wt.%), O (44.23 wt.%), C (16.06 wt.%) Na (0.61 wt.%), Cl (0.70 wt.%) and Mg (0.54 wt.%) in the formed apatite nanocrystals. High level of bioactivity of the as-prepared nHA may be due to the beneficial effects of Mg as well as carbonates [29–33]. Carbonate is one of the most abundant ions (4–8 wt%) present in bone apatite [27,28] and it plays an essential role on bone resorption and formation [29–33]. Carbonated HA have improved bioactivity than pure HA because incorporation of carbonate into HA caused an increase in solubility and increases the local concentration of calcium and phosphate ions that are necessary for the formation of bone-like apatite [29–33]. Also Mg is one of the important trace elements present in calcified tissues and it plays a key role in bone metabolism, in particular during the early stages of osteogenesis [29,31]. Moreover, nano sized HA have better bioactivity than coarser crystals [1,9]. Therefore, not only the presence of Mg and carbonate in nHA but their morphology and size are also responsible for higher bioactivity of nHA.

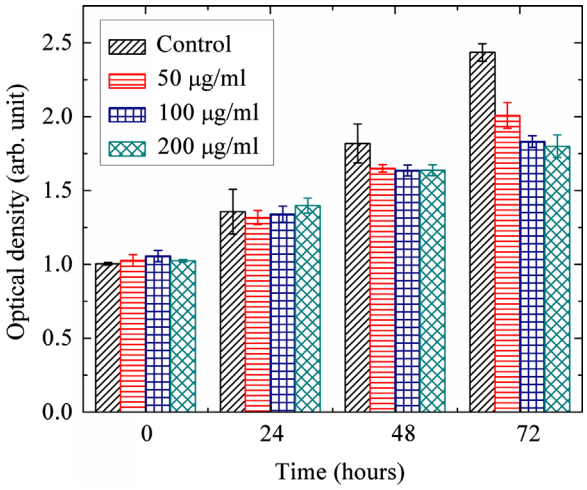

Fig. 3. Growth activity of mouse fibroblast 3T3-L1 cells for different dosages of nHA.

In vitro models based on cell cultures provide useful information regarding material biocompatibility [34]. Fig. 3 shows the growth activity of mouse fibroblast 3T3-L1 cells with different dosages of nHA after different incubation periods. A significant increase in the growth of mouse fibroblast 3T3-L1 cells with culture time was observed which confirmed the excellent biocompatibility of the prepared nHA.

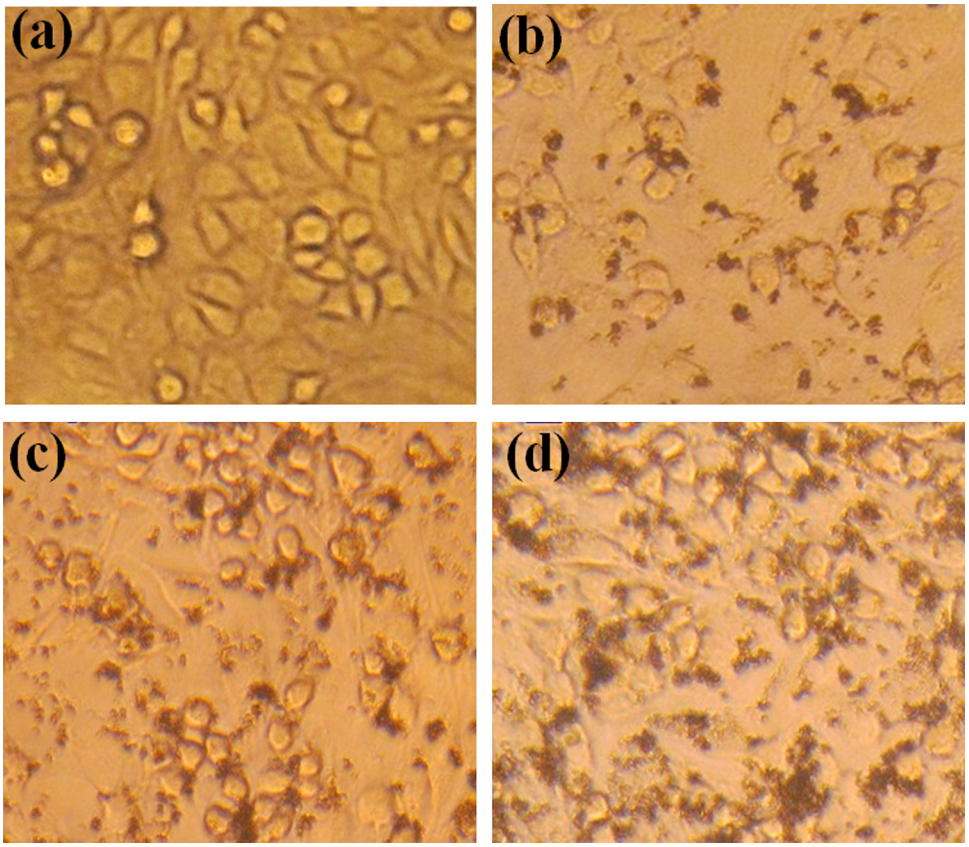

Fig. 4. Optical image of (a) mouse fibroblast 3T3-L1 cells (b) cells contained 50 μg/ml of nHA (c) cells contained 100 μg/ml of nHA (d) cells contained 200 μg/ml of nHA, after 72 h incubation.

However, growth rate of nHA added cells are low when compared with the control. It is noted that up to 48 h, no significant difference was observed between the growth rates of nHA added cells. On further incubation, cell growth decreased with increasing nHA dosage. Optical image of mouse fibroblast 3T3-L1 cells and cells contained different dosages of nHA for 72 h incubation is shown in Fig. 4.

HA can be ascribed to the category of non-swellable and non-resorbable drug delivery matrix. Thus the drug molecules can be adsorbed onto the surface of HA during the process of drug loading [35–37]. The UV–vis analysis demonstrate that the prepared nHA have the drug loading efficiency of about 28.3% for doxycycline hydrochloride. Since doxycycline contains electron-donor groups likely to generate stable complexes with Ca^{2+}, thus presenting a strong affinity for its adsorption on HA [25]. The cumulative drug release profiles of doxycycline hydrochloride loaded nHA as a function of release time in PBS medium is shown in Fig. 5. The profile of drug release comprises an initial burst release (about 60% for 6 h) followed by a slow release (about 8% for last 54 h). The initial burst release may be caused by desorption of weakly adsorbed drug molecules on the surface of nHA whereas the slow release of the remaining drug may be caused by desorption of the strongly adsorbed drug molecules.

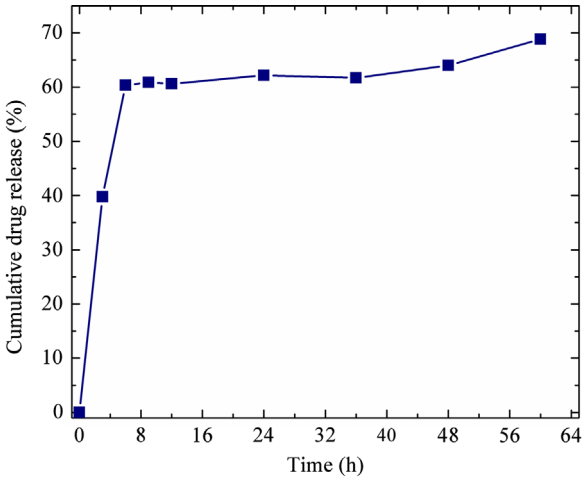

Fig. 5. Cumulative doxycycline hydrochloride release from drug loaded HA nanocarrier as a function of release time in the release media of PBS.

One of the major problems after surgery is bacterial infection. Antibiotics are often used to fight against the bacterial infection [38]. It is highly preferred that there is an initial burst release of the antibiotics from the carrier immediately after surgery for efficient inhibition of micro-organisms and then a sustained release provides continuous delivery of the drug at the site of infection for a long term treatment [17]. Generally, the profile of drug or protein release from HA ceramics comprises an initial rapid burst followed by a plateau at longer times and it is a great challenge to sustain the release and decrease the initial burst release of drugs as well as proteins from HA [10–12]. Polymer encapsulation on prepared nHA nanostructure may control the rate of drug release and extend the period of drug release [11,12,25]. Therefore, further investigation is needed to reduce the burst release and increase sustained release of drug molecules from the prepared nHA.

Doxycycline hydrochloride is a broad spectrum tetracycline antibiotic, which is commonly used in the treatment of dental, periodontal and bone related infections caused by bacteria [39]. Antibacterial activity of nHA and doxycycline hydrochloride loaded nHA (DL-nHA) against *E. coli* and *B. cereus* is shown in Fig. 6. There is no inhibition zone around the nHA. Drug loaded nHA showed inhibition zone around the pellet in which bacterial growth is inhibited with a diameter of 20 ± 0.5 mm and 08 ± 0.5 mm for *E. coli* and *B. cereus*, respectively. Bacteria must synthesize proteins in order to ensure their growth. Doxycycline hydrochloride penetrates the bacterial cell and blocks the protein synthesis which inhibits the growth of bacteria [40,41]. These results evidenced the antibacterial activity of doxycycline hydrochloride against *E. coli* and *B. cereus* and are of great interest either to prevent infections produced surgical interventions, or in the treatment of bone related infections.

PL emission spectrum of as-synthesized nHA is shown in Fig. 7. It shows a strong emission consisting of a broad band

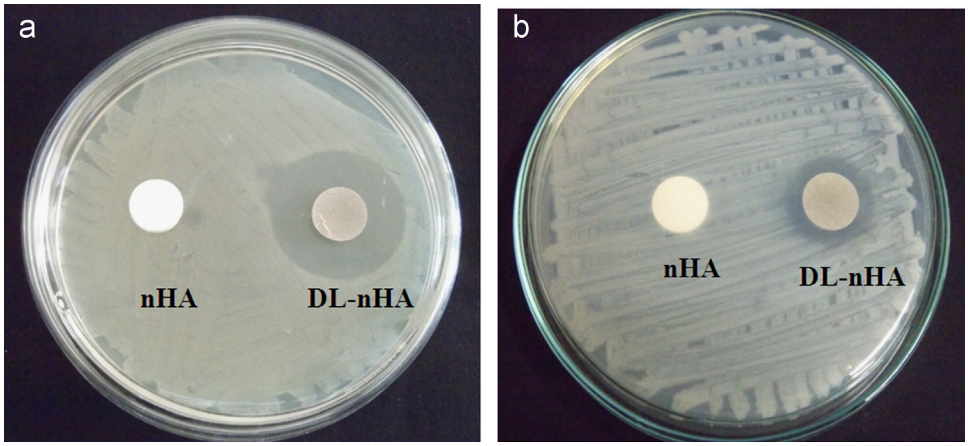

Fig. 6. Antibacterial activity of nHA and doxycycline hydrochloride loaded HA (DL-nHA) against (a) *Escherichia coli* and (b) *Bacillus cereus*.

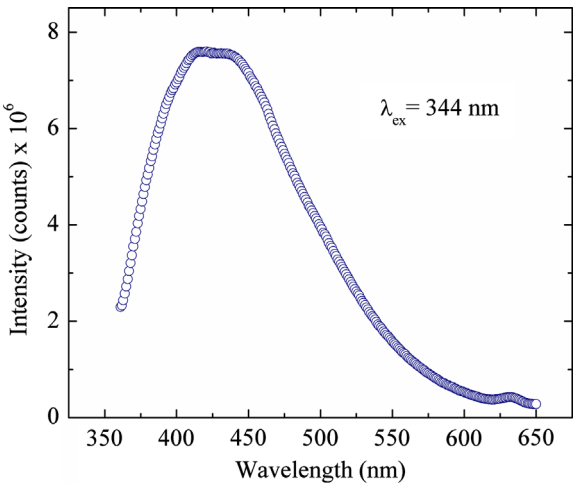

Fig. 7. PL emission spectrum of as-synthesized nHA (Excitation wavelength is λ_{ex}=344 nm).

between 360 nm and 550 nm with maximum around 430 nm. Generally, pure HA does not show any luminescence properties whereas transition metal and rare earth ions substituted HA showed very interesting luminescent properties which make them useful for biological fluorescent labeling. However, carbonate related impurities may also provide self-activated luminescence property to HA [8,42–46]. Zhang et al. reported that the self activated luminescence emission of HA might result from the $CO_2^{\bullet-}$ radicals as impurities which were formed during the synthesis of HA in the presence of citric acid [44]. Also, Sepahvandi et al. reported that the carbonate related impurities are responsible for the luminescence emission of biomimetic apatite coatings formed on Ti substrate [42]. Whereas the prepared nHA in the present study is B-type carbonated HA which showed an excellent luminescent blue emission. B-type carbonate substitution in HA yields a substoichometry in calcium site, in order to achieve the charge compensation. The charge imbalance associated with the two CO_3^{2-} ions substitution for phosphate can be compensated by a single Ca vacancy as follows

$$Ca^{2+}+2PO_4^{3-}\leftrightarrow V_{Ca}+2CO_3^{2-}$$

where, V_{Ca} represents a Ca vacancy site [30]. Therefore, observed luminescence may be due to some carbonate impurities and/or defects present in the structure of nHA which act as a luminescent center and resulted in blue emission [42–46]. Consequently prepared nHA can be a potential luminescent material for the development of novel biocompatible probes.

4. Conclusions

In vitro studies and photoluminescence characterization were carried out on flower-like HA nanostructure (nHA) which was obtained from eggshell biowaste. The obtained nHA exhibited good apatite forming ability in SBF and excellent biocompatibility with mouse fibroblast 3T3-L1 cells. Moreover, doxycycline hydrochloride loaded nHA showed burst releasing feature and an excellent antibacterial activity against *E. coli* and *B. cereus*. Besides, it exhibits inherent luminescence property. In view of these interesting properties the flower like nHA obtained from the eggshell waste may be a potential candidate for the development of drug delivery carriers, bone substitutes and bioprobes.

Acknowledgments

This work was financially supported by Department of Science and Technology, India through project (Project Ref. no.: SR/FTP/PS-24/2009). One of the authors G. Suresh Kumar acknowledges the Council of Scientific and Industrial Research (CSIR), India for the award of Senior Research Fellowship (File no.: 09/810(0016)/2012-EMR-I). The discussions with Dr. A. Thamizhavel, Tata Institute of Fundamental Research are gratefully acknowledged.

References

[1] S.V. Dorozhkin, Nanosized and nanocrystalline calcium orthophosphates, Acta Biomaterialia 6 (2010) 715–734.
[2] Y. Hong, H. Fan, B. Li, B. Guo, M. Liu, X. Zhang, Fabrication, biological effects and medical applications of calcium phosphate nanoceramics, Materials Science and Engineering R 70 (2010) 225–242.
[3] S.R. Paital, N.B. Dahotre, Calcium phosphate coatings for bio-implant applications: materials, performance factors and methodologies, Materials Science and Engineering R 66 (2009) 1–70.
[4] V.S. Bystrov, E. Paramonova, Y. Dekhtyar, A. Katashev, A. Karlov, N. Polyaka, A.V. Bystrova, A. Patmalnieks, A.L. Kholkin, Computational and experimental studies of size and shape related physical properties of hydroxyapatite nanoparticles, Journal of Physics: Condensed Matter 23 (2011) 065302.
[5] Z. Shi, X. Huang, Y. Cai, R. Tang, D. Yang, Size effect of hydroxyapatite nanoparticles on proliferation and apoptosis of osteoblast-like cells, Acta Biomaterialia 5 (2009) 338–345.
[6] J. Song, Y. Liu, Y. Zhang, L. Jiao, Mechanical properties of hydroxyapatite ceramics sintered from powders with different morphologies, Materials Science and Engineering A 528 (2011) 5421–5427.
[7] S. Roohani-Esfahani, S. Nouri-Khorasani, Z. Lu, R. Appleyard, H. Zreiqat, The influence hydroxyapatite nanoparticle shape and size on the properties of biphasic calcium phosphate scaffolds coated with hydroxyapatite–PCL composites, Biomaterials 31 (2010) 5498–5509.
[8] C. Zhang, J. Yang, Z. Quan, P. Yang, C. Li, Z. Hou, J. Lin, Hydroxyapatite nano- and microcrystals with multiform morphologies: controllable synthesis and luminescence properties, Crystal Growth and Design 9 (2009) 2725–2733.
[9] M. Vallet-Regi, D. Arcos, in: Biomimetic Nanoceramics in Clinical Use: From Materials to Applications, First ed., RSC Publishing, Cambridge, 2008.
[10] L. Yang, J. Yin, L. Wang, G. Xing, P. Yin, Q. Liu, Hydrothermal synthesis of hierarchical hydroxyapatite: preparation, growth mechanism and drug release property, Ceramics International 38 (2012) 495–502.
[11] W. Paul, C.P. Sharma, Development of porous spherical hydroxyapatite granules: application towards protein delivery, Journal of Materials Science: Materials in Medicine 10 (1999) 383–388.
[12] Y. Wang, M.S. Hassan, P. Gunawan, R. Lau, X. Wang, R. Xu, Polyelectrolyte mediated formation of hydroxyapatite microspheres of controlled size and hierarchical structure, Journal of Colloid and Interface Science 339 (2009) 69–77.
[13] M. Chen, D. Jiang, D. Li, J. Zhu, G. Li, J. Xie, Controllable synthesis of fluorapatite nanocrystals with various morphologies: effects of pH value and chelating reagent, Journal of Alloys and Compounds 485 (2009) 396–401.

[14] P.M.S.L. Shanthi, R.V. Mangalaraja, A.P. Uthirakumar, S. Velmathi, T. Balasubramanian, M. Ashok, Synthesis and characterization of porous shell-like nano hydroxyapatite using cetrimide as template, Journal of Colloid and Interface Science 350 (2010) 39–43.
[15] A. Bigi, E. Boanini, K. Rubini, Hydroxyapatite gels and nanocrystals prepared through a sol–gel process, Journal of Solid State Chemistry 177 (2004) 3092–3098.
[16] E.K. Girija, G.S. Kumar, A. Thamizhavel, Y. Yokogawa, S.N. Kalkura, Role of material processing on the sinterability and thermal stability of nanocrystalline hydroxyapatite, Powder Technology 225 (2012) 190–195.
[17] R. Vani, S.B. Raja, T.S. Sridevi, K. Savithri, S.N. Devaraj, E.K. Girija, A. Thamizhavel, S.N. Kalkura, Surfactant free rapid synthesis of hydroxyapatite nanorods by a microwave irradiation method for the treatment of bone infection, Nanotechnology 22 (2011) 285701.
[18] J. Liu, K. Li, H. Wang, M. Zhu, H. Yan, Rapid formation of hydroxyapatite nanostructures by microwave irradiation, Chemical Physics Letters 396 (2004) 429–432.
[19] A. Lopez-Macipe, J. Gomez-Morales, R. Rodriguez-Clemente, Nanosized hydroxyapatite precipitation from homogeneous calcium/citrate/phosphate solutions using microwave and conventional heating, Advanced Materials 10 (1998) 49–53.
[20] H. Arami, M. Mohajerani, M. Mazloumi, R. Khalifehzadeh, A. Lak, S. K. Sadrnezhaad, Rapid formation of hydroxyapatite nanostrips via microwave irradiation, Journal of Alloys and Compounds 469 (2009) 391–394.
[21] E.M. Rivera, M. Araiza, W. Brostow, V.M. Castano, J.R. Diaz-Estrada, R. Hernandez, J.R. Rodriguez, Synthesis of hydroxyapatite from eggshells, Materials Letters 41 (1999) 128–134.
[22] G.S. Kumar, A. Thamizhavel, E.K. Girija, Microwave conversion of eggshells into flower-like hydroxyapatite nanostructure for biomedical applications, Materials Letters 76 (2012) 198–200.
[23] A.C. Tas, Synthesis of biomimetic Ca-hydroxyapatite powders at 37 °C in synthetic body fluids, Biomaterials 21 (2000) 1429–1438.
[24] J. Carmichael, W.G. DeGraff, A.F. Gazdar, J.D. Minna, J.B. Mitchell, Evaluation of a tetrazolium-based semiautomated colorimetric assay: assessment of chemosensitivity testing, Cancer Research 47 (1987) 936–942.
[25] S. Wang, X. Wang, H. Xu, H. Abe, Z. Tan, Y. Zhao, J. Guo, M. Naito, H. Ichikawa, Y. Fukumori, Towards sustained delivery of small molecular drugs using hydroxyapatite microspheres as the vehicle, Advanced Powder Technology 21 (2010) 268–272.
[26] R. Murugan, S. Ramakrishna, Designing biological apatite suitable for neomycin delivery, Journal of Materials Science 41 (2006) 4343–4347.
[27] R.Z. LeGeros, Calcium Phosphates in Oral Biology and Medicine, Karger, Basel, Switzerland, 1991.
[28] S.V. Dorozhkin, Calcium orthophosphates in nature, biology and medicine, Materials 2 (2009) 399–498.
[29] E. Boanini, M. Gazzano, A. Bigi, Ionic substitutions in calcium phosphates synthesized at low temperature, Acta Biomaterialia 6 (2010) 1882–1894.
[30] G.S. Kumar, A. Thamizhavel, Y. Yokogawa, S.N. Kalkura, E.K. Girija, Synthesis, characterization and *in vitro* studies of zinc and carbonate co-substituted nano-hydroxyapatite for biomedical applications, Materials Chemistry and Physics 134 (2012) 1127–1135.
[31] E. Landi, A. Tampieri, M. Mattioli-Belmonte, G. Celotti, M. Sandri, A. Gigante, P. Fava, G. Biagini, Biomimetic Mg- and Mg, CO_3-substituted hydroxyapatites: synthesis characterization and *in vitro* behavior, Journal of the European Ceramic Society 26 (2006) 2593–2601.
[32] A. Porter, N. Patel, R. Brooks, S. Best, N. Rushton, W. Bonfield, Effect of carbonate substitution on the ultrastructural characteristics of hydroxyapatite implants, Journal of Materials Science: Materials in Medicine 16 (2005) 899–907.
[33] E.S. Kovaleva, M.P. Shabanov, V.I. Putlyaev, Y.D. Tretyakov, V. K. Ivanov, N.I. Silkin, Bioresorbable carbonated hydroxyapatite $Ca_{10-x}Na_x(PO_4)_{6-x}(CO_3)_x(OH)_2$ powders for bioactive materials preparation, Central European Journal of Chemistry 7 (2009) 168–174.
[34] M. Vallet-Regi, D. Arcos, Silicon substituted hydroxyapatites. A method to upgrade calcium phosphate based implants, Journal of Materials Chemistry 15 (2005) 1509–1516.
[35] S. Bose, S. Tarafder, Calcium phosphate ceramic systems in growth factor and drug delivery for bone tissue engineering: a review, Acta Biomaterialia 8 (2012) 1401–1421.
[36] W. Ji, H. Wang, J.J.J.P. van den Beucken, F. Yang, X.F. Walboomers, S. Leeuwenburgh, J.A. Jansen, Local delivery of small and large biomolecules in craniomaxillofacial bone, Advanced Drug Delivery Reviews 64 (2012) 1152–1164.
[37] P. Yang, Z. Quan, C. Li, X. Kang, H. Lian, J. Lin, Bioactive, luminescent and mesoporous europium-doped hydroxyapatite as a drug carrier, Biomaterials 29 (2008) 4341–4347.
[38] C. Castro, E. Sanchez, A. Delgado, I. Soriano, P. Nunez, M. Baro, A. Perera, C. Evora, Ciprofloxacin implants for bone infection. *In vitro–in vivo* characterization, Journal of Controlled Release 93 (2003) 341–354.
[39] F. Tamimi, J. Torres, R. Bettini, F. Ruggera, C. Rueda, M. Lopez-Ponce, E. Lopez-Cabarcos, Doxycycline sustained release from brushite cements for the treatment of periodontal diseases, Journal of Biomedical Materials Research A 85 (2008) 707–714.
[40] ⟨http://www.cbwinfo.com/Pharmaceuticals/Doxycycline.html⟩.
[41] ⟨http://www.emedexpert.com/facts/doxycycline-facts.shtml⟩.
[42] A. Sepahvandi, F. Moztarzadeha, M. Mozafari, M. Ghaffari, N. Raee, Photoluminescence in the characterization and early detection of biomimetic bone-like apatite formation on the surface of alkaline-treated titanium implant: state of the art, Colloids and Surfaces B: Biointerfaces 86 (2011) 390–396.
[43] C. Zollfrank, L. Muller, P. Greil, F.A. Muller, Photoluminescence of annealed biomimetic apatites, Acta Biomaterialia 1 (2005) 663–669.
[44] C. Zhang, C. Li, S. Huang, Z. Hou, Z. Cheng, P. Yang, C. Peng, J. Lin, Self-activated luminescent and mesoporous strontium hydroxyapatite nanorods for drug delivery, Biomaterials 31 (2010) 3374–3383.
[45] R. Chung, T.S. Chin, H. Cheng, H. Wen, M. Hsieh, Photo-luminescent hydroxyapatite coatings through a bio-mimetic process, Biomolecular Engineering 24 (2007) 459–461.
[46] C. Zhang, J. Lin, Defect-related luminescent materials: synthesis, emission properties and applications, Chemical Society Reviews 41 (2012) 7938–7961.